AIAA 2002-4300

ASSESSMENT OF VARIOUS FLOW SOLVERS USED TO PREDICT THE THERMAL ENVIRONMENT INSIDE SPACE SHUTTLE SOLID ROCKET MOTOR JOINTS

Qunzhen Wang
ATK Thiokol Propulsion
P.O. Box 707, M/S 252
Brigham City, UT 84302

38th AIAA/ASME/SAE/ASEE
Joint Propulsion Conference and Exhibit
July 7-10, 2002
Indianapolis, Indiana

Assessment of Various Flow Solvers Used to Predict the Thermal Environment Inside Space Shuttle Solid Rocket Motor Joints

Qunzhen Wang[§]
ATK Thiokol Propulsion Corp., Brigham City, UT

INTRODUCTION

It is very important to accurately predict the gas pressure, gas and solid temperature, as well as the amount of O-ring erosion inside the space shuttle Reusable Solid Rocket Motor (RSRM) joints in the event of a leak path. The scenarios considered are typically hot combustion gas rapid pressurization events of small volumes through narrow and restricted flow paths. The ideal method for this prediction is a transient three-dimensional computational fluid dynamics (CFD) simulation with a computational domain including both combustion gas and surrounding solid regions. However, this has not yet been demonstrated to be economical for this application due to the enormous amount of CPU time and memory resulting from the relatively long fill time as well as the large pressure and temperature rising rate. Consequently, all CFD applications in RSRM joints so far[1,2] are steady-state simulations with solid regions being excluded from the computational domain by assuming either a constant wall temperature or no heat transfer between the hot combustion gas and cool solid walls.

The complicated gas dynamics, heat transfer, and O-ring erosion phenomena in the RSRM joint pressurization process are currently modeled by two widely used computer codes. One is SFLOW[3,4], which was recently developed at ATK Thiokol Propulsion, and the other is JPR[5,6], which was developed by NASA Marshall Space Flight Center. While both codes apply SINDA/G[7], a commercial thermal analyzer, to calculate the solid temperature for a given heat flux, the flow solvers used to model the transient compressible flows are very different. Before SFLOW was developed, a code called ORING2[8] and its previous version ORING had been widely used at ATK Thiokol Propulsion to predict the thermal-flow environment at various RSRM joints. The major difference between these codes is also the flow solver used to calculate the pressure, temperature, and Mach number of the gas as well as the heat flux from the hot combustion gas to the surrounding cold solid parts.

The flow of high pressure and high temperature combustion gas from the RSRM combustion chamber to the O-ring grove inside various joints is a highly transient compressible process involving flow area change, friction, heat transfer from the hot gas to cold solid walls, as well as the mass addition due to the flow path and O-ring erosion. The main objective of this paper is to assess the capability of various flow solvers, which have been used in simulating the thermal environments of RSRM joints, to accurately predict transient compressible flow phenomena with area change, friction, heat transfer, and mass addition. Besides the flow solvers used in SFLOW, ORING2, ORING and JPR, another flow solver is studied where the governing equation is the generalized one-dimensional steady flow equation taking into account the effects of area change, friction, heat transfer and mass addition[9]. Specifically, the following five flow solvers have been incorporated into SFLOW to study their capability in accurately predicting the transient compressible flows with area change, friction, heat transfer and mass addition: (1) isentropic method, (2) ORING2 method, (3) Lapple[10] method, (4) generalized method, and (5) SHARP[11-13] method. Note that, although SHARP can perform two-dimensional as well as three-dimensional CFD simulations, only the one-dimensional part is considered in this paper. The other four solvers are for one-dimensional flows only.

The following test cases with exact solutions are used to assess the above flow solvers: (1) steady flow with area change, (2) steady flow with friction, (3) steady flow with heat transfer, (4) steady flow with mass addition,

[§]Sr. Principal Engineer, Gas Dynamics, AIAA member

(5) transient flow with area change, (6) transient flow with heat transfer, (7) transient flow with area change, friction, and heat transfer, and (8) volume filling.

The details of various flow solvers are discussed in next section followed by the comparison of predictions from various flow solvers with the exact solutions.

NUMERICAL METHODS

Isentropic Method

For steady isentropic flow in a pipe, the ratio of critical pressure to inlet stagnation pressure is

$$\frac{p^*}{p_0} = \left(\frac{2}{\gamma+1}\right)^{\frac{\gamma}{\gamma-1}} \tag{1}$$

where γ is the ratio of specific heats. If the ratio of back pressure to inlet stagnation pressure p_b/p_0 is larger than this critical pressure ratio, the flow is not choked and the mass flow rate is obtained from

$$\dot{m} = C_d \rho_e V_e A_e \tag{2}$$

where ρ_e, V_e and A_e are the density, velocity and cross-section area at the pipe exit, respectively. The discharge coefficient C_d accounts for the non-isentropic effects on the mass flow rate such as friction. The gas properties at the pipe exit can be calculated as

$$\rho_e = \rho_0 \left(1 + \frac{\gamma-1}{2} M_e^2\right)^{-\frac{1}{\gamma-1}} \tag{3}$$

$$V_e = M_e \sqrt{\gamma R T_e} \tag{4}$$

$$M_e = \sqrt{\frac{2}{\gamma-1}\left[\left(\frac{p_0}{p_b}\right)^{\frac{\gamma-1}{\gamma}} - 1\right]} \tag{5}$$

$$T_e = T_0 \left(1 + \frac{\gamma-1}{2} M_e^2\right)^{-1} \tag{6}$$

where R is the gas constant, ρ_0 and T_0 are the stagnation density and temperature at the pipe inlet, respectively. Substituting equations (3) and (6) into equation (2) yields

$$\dot{m} = \frac{C_d p_0 A_e}{\sqrt{R T_0}} \sqrt{\frac{2\gamma}{\gamma-1}\left(\frac{p_b}{p_0}\right)^{2/\gamma}\left[1 - \left(\frac{p_b}{p_0}\right)^{(\gamma-1)/\gamma}\right]} \tag{7}$$

If the pressure ratio p_b/p_0 is smaller than the critical pressure ratio, the flow is choked and the mass flow rate is obtained from

$$\dot{m} = \frac{C_d p_0 A_e}{\sqrt{R T_0}} \sqrt{\gamma}\left(\frac{2}{\gamma+1}\right)^{\frac{\gamma+1}{2(\gamma-1)}} \tag{8}$$

Note that equation (8) can be obtained by replacing p_b/p_0 in equation (7) with the critical pressure ratio in equation (1).

ORING2 Method

While the isentropic method discussed in the last section applies a discharge coefficient to account for nonisentropic effects such as friction, the ORING2 method eliminates the discharge coefficient and introduces a form loss parameter K. For flows with friction loss only,

$$K = \frac{fL}{D} \tag{9}$$

where D is the hydraulic diameter and L is the length of the flow path. The Darcy friction factor is defined as

$$f = \frac{\tau_w}{\frac{1}{8}\rho V_m^2} \tag{10}$$

where τ_w is the wall shear stress and V_m is the bulk velocity inside the flow path. In general, the loss parameter K should also include pressure loss due to sudden expansion or contraction and turns or bends in the flow path.

In the ORING2 method, the critical pressure ratio is calculated as

$$\frac{p^*}{p_0} = \left(1 - \frac{\frac{\gamma-1}{2} M_c^2 (1+K)}{1 + \frac{\gamma-1}{2} M_c^2}\right)^{\frac{\gamma}{\gamma-1}} \tag{11}$$

where the choked Mach number is obtained from

$$M_c = \sqrt{\frac{-B-\sqrt{B^2-4AC}}{2A}} \tag{12}$$

$$A = \frac{1}{1+K} - 1 \tag{13}$$

$$C = \frac{2}{(1+K)(\gamma-1)^2} \tag{14}$$

$$B = \frac{3}{(1+K)(\gamma-1)} - \frac{3\gamma-1}{(\gamma-1)^2} \tag{15}$$

If the ratio of back pressure to inlet stagnation pressure p_b/p_0 is larger than the critical pressure ratio in equation (11), the flow is not choked and the Mach number at the pipe exit is

$$M_e = \sqrt{\frac{2}{\gamma-1}\frac{1}{1+K}\frac{1-\left(\frac{p_b}{p_0}\right)^{\frac{\gamma-1}{\gamma}}}{1-\frac{1}{1+K}\left(1-\left(\frac{p_b}{p_0}\right)^{\frac{\gamma-1}{\gamma}}\right)}} \tag{16}$$

The mass flow rate is then obtained from

$$\dot{m} = \frac{p_0 A_e}{\sqrt{RT_0}} \frac{M\left(1-\frac{\gamma-1}{2}KM^2\right)^{\frac{\gamma}{\gamma-1}}}{\sqrt{\frac{1}{\gamma}\left(1+\frac{\gamma+1}{2}M^2\right)^{\frac{\gamma+1}{2(\gamma-1)}}}} \tag{17}$$

The Mach number M in equation (17) is the choked Mach number M_c if the back pressure to inlet stagnation pressure p_b/p_0 is smaller than the critical pressure ratio and is the unchoked Mach number M_e if the flow is not choked. It can be shown that, for flows with no form loss (i.e., K=0), equation (17) is identical to equations (7) and (8) of the isentropic method.

Note that the ORING2 method does not take into account the effects of heat transfer and mass addition when the mass flow rate is calculated using equation (17). Note also that, in real problems, the loss factor is usually a function of mass flow rate and, thus, an iteration method has to be applied to calculate the mass flow rate from equation (17). In SFLOW, a loss factor is first guessed and then equation (17) is used to calculate the mass flow rate. A new loss factor is obtained from this mass flow rate and equation (17) is applied again to obtain a new mass flow rate. This process is repeated until the form loss and mass flow rate are converged.

Lapple Method

For steady adiabatic flows in a pipe with constant cross-section area and no mass addition, Lapple[10] derived a method to calculate the mass flow rate as

$$\dot{m} = \frac{p_0 A_e}{\sqrt{RT_0}} f\left(K, \gamma, \frac{p_b}{p_0}\right) \tag{18}$$

A table was developed for the mass flow rate at different loss factor K, ratio of specific heats γ, and pressure ratio p_b/p_0. This Lapple table only lists mass flow rate for K up to 200. In some applications such as the carbon fiber rope[4], however, the friction factor is usually very large and K could be as large as 10^6. Thus, the Lapple table is extended in SFLOW for large values of K based on the asymptotic relationship

$$\dot{m} = \frac{p_0 A_e}{\sqrt{RT_0}}\sqrt{\frac{1}{K}} \qquad for \quad K \to \infty \tag{19}$$

In particular, for K>200, the mass flow rate is calculated by

$$\dot{m} = \frac{p_0 A_e}{\sqrt{RT_0}}\sqrt{\frac{1}{K}}\left(1-\frac{p_b}{p_0}\right)^{0.1522-0.0451 p_b/p_0+0.3275(p_b/p_0)^2} \tag{20}$$

The constants in this equation are obtained by curve fitting using the least-square method.

Note that, similar to the ORING2 method, iteration methods should also be applied for calculating the mass flow rate due to the fact that the loss factor usually depends on the mass flow rate. The Lapple method also does not take into account the effects of heat transfer and mass addition when the mass flow rate is calculated.

Figure 1 and Figure 2 show the mass flow rate for different pressure ratios as well as loss factors. The ratio of specific heats used in these figures is 1.4. As expected, the flow rate increases with decreasing friction and with decreasing pressure ratio but the flow rate is constant for very large friction or small back pressure due to choking.

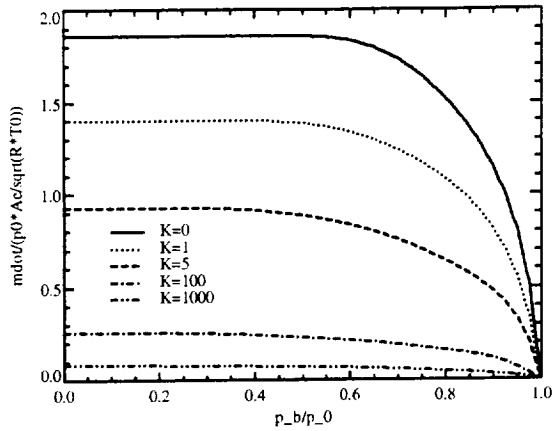

Figure 1: Mass flow rate vs. pressure ratio for different loss factors in the Lapple method.

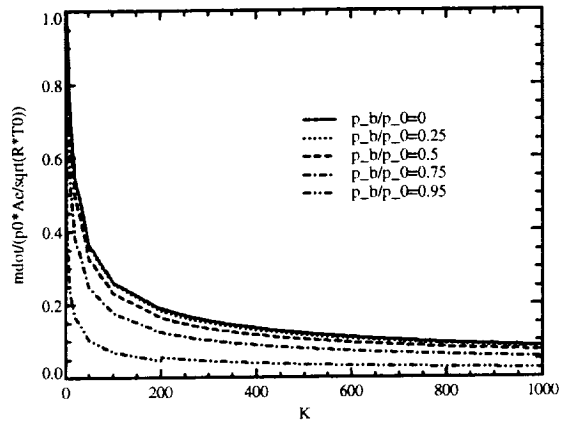

Figure 2: Mass flow rate vs. loss factor for different pressure ratios in the Lapple method.

Figure 3 compares mass flow rate vs. pressure ratio for isentropic and Lapple methods when there is no pressure loss (i.e., K=0). The specific heat ratio used is 1.4 and the discharge coefficient is 1.0. Both methods predict the same mass flow rate for choked flow when p_b/p_0<0.53 and no flow for p_b/p_0 =1. For unchoked flow with 0.9<p_b/p_0<1, however, the mass flow rate predicted by the Lapple method is slightly smaller than that from the isentropic method. This is because the Lapple table does not list mass flow rate for 0.9<p_b/p_0<1 and curve fitting is used in SFLOW to calculate mass flow rate at this pressure range, where the mass flow rate decreases dramatically with increasing pressure ratio. Note that, as discussed above, the mass flow rate from the ORING2 method, equation (17), when K=0 is the same as that from the isentropic method.

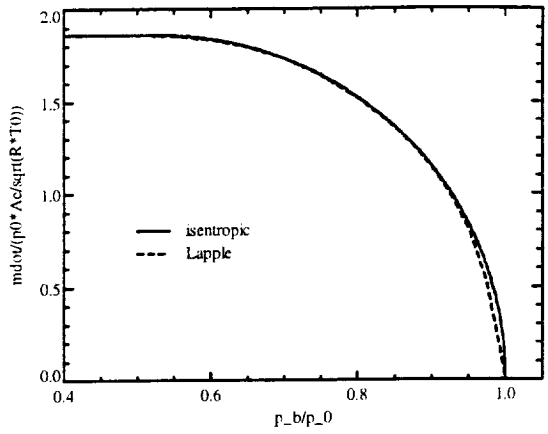

Figure 3: Comparison of mass flow rate vs. pressure ratio for isentropic and Lapple methods.

The mass flow rate vs. pressure ratio from ORING2 and Lapple methods for different loss factors are compared in Figure 4 and Figure 5 with a specific heat ratio of 1.4. In general, the ORING2 method predicts a mass flow rate smaller than that from the Lapple method.

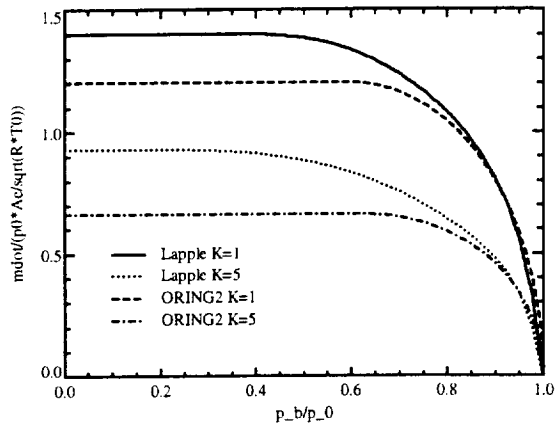

Figure 4: Comparison of mass flow rate vs. pressure ratio from ORING2 and Lapple methods for K=1 and K=5.

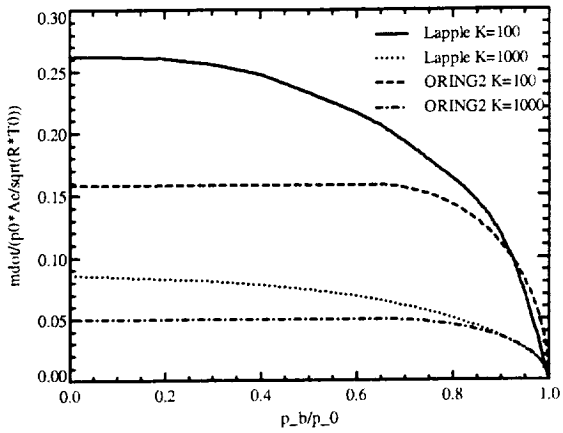

Figure 5: Comparison of mass flow rate vs. pressure ratio from ORING2 and Lapple methods for K=100 and K=1000.

Generalized Method

Both the ORING2 and Lapple methods discussed above do not take into account the effects of heat transfer and mass addition when the mass flow rate is calculated. A generalized steady flow equation relating the Mach number and area change, friction, heat transfer as well as mass addition parameters can be derived as

$$\frac{dM}{M} = \frac{1+\frac{\gamma-1}{2}M^2}{1-M^2}\left[-\frac{dA}{A}+\frac{\gamma M^2}{2}\frac{f\,dx}{D}+\frac{1+\gamma M^2}{2}\frac{dT_0}{T_0}+\left(1+\gamma M^2\right)\frac{d\dot{m}}{\dot{m}}\right] \quad (21)$$

Once the Mach number at every flow cells is obtained by solving this ordinary differential equation, the pressure and temperature at cell $i+1$ can be calculated from

$$p_{i+1} = p_i \frac{\dot{m}_{i+1}}{\dot{m}_i}\frac{A_i}{A_{i+1}}\frac{M_i}{M_{i+1}}\sqrt{\frac{T_{0,i+1}\left(1+\frac{\gamma-1}{2}M_i^2\right)}{T_{0,i}\left(1+\frac{\gamma-1}{2}M_{i+1}^2\right)}} \quad (22)$$

$$T_{i+1} = \frac{T_{0,i+1}\left(1+\frac{\gamma-1}{2}M_i^2\right)}{T_{0,i}\left(1+\frac{\gamma-1}{2}M_{i+1}^2\right)}T_i \quad (23)$$

The stagnation temperature and mass flow rate at cell $i+1$ can be obtained from the heat transfer and the mass addition to the gas using energy and mass conservations laws

$$T_{0,i+1} = T_{0,i} + \frac{q_i}{c_p} \quad (24)$$

$$\dot{m}_{i+1} = \dot{m}_i + \dot{m}_{a,i} \quad (25)$$

where q_i and $\dot{m}_{a,i}$ are the heat transfer and mass addition to the gas at cell i. For a real problem, the inlet Mach number is usually unknown and the known values are the stagnation pressure and temperature at the inlet and the back pressure at the outlet. Moreover, the friction factor, heat transfer, and mass addition are often functions of mass flow rate. Therefore, an iteration method has to be applied to calculate flow properties using the generalized method. In SFLOW, the inlet Mach number is first guessed, the friction factor, heat transfer, and mass addition are then evaluated. Next, equation (21) is solved for Mach number at every flow cells using the forth-order Runge-Kutta method. Finally, the pressure and temperature at every cell are calculated from equations (22) and (23). The process is repeated until the outlet pressure matches the known value.

SHARP Method

All the methods discussed above are derived for steady flow problems. The transient compressible flow in a path can be modeled using SHARP[11-13], which is a general-purpose CFD code. While SHARP can also solve two-dimensional as well as three-dimensional flow problems, only one-dimensional flows are considered in this paper. In one-dimensional flow problems, SHARP solves the Navier-Stokes equation as

$$\frac{\partial Q}{\partial t}+\frac{\partial E}{\partial x} = S \quad (26)$$

where the unknowns are

$$Q = A\begin{bmatrix}\rho\\ \rho u\\ e\end{bmatrix} \quad (27)$$

where ρ and u are the gas density and velocity, respectively. The total energy is

$$e = \rho\left(c_v T + \frac{1}{2}u^2\right) \tag{28}$$

where T is the gas temperature and c_v is the specific heat at constant volume. The inviscid flux term is given by

$$E = A\begin{bmatrix} \rho u \\ \rho u^2 + p \\ (e+p)u \end{bmatrix} \tag{29}$$

The source term in equation (26) is

$$S = \begin{bmatrix} \frac{\dot{m}_a A}{V} \\ -\frac{fA\rho u|u|}{2D} \\ -\dot{q}\frac{A}{V} - \frac{fA\rho|u|^3}{2D} \end{bmatrix} \tag{30}$$

where V is the volume of the flow cell.

Note that, unlike the other solvers, both SHARP and generalized methods do not solve the mass flow rate directly. Instead, the Mach number, pressure, and temperature in the flow path are calculated and the mass flow rate can then be obtained as $\dot{m} = \rho A u$. Note also that the predicted mass flow rate from SHARP is not necessary constant at different cells of a flow path whereas all other four methods predict the same mass flow rate at different cells.

Pressure, Temperature, Mach number in Flow Path

The isentropic, Lapple and ORING2 methods only give a way to calculate the mass flow rate in the flow path. For the solid rocket joint simulations, the pressure, temperature and Mach number in the flow path are also needed to calculate the heat transfer from the hot combustion gas to the cold solid surfaces. In this paper, the pressure, temperature and Mach number in the flow path for these methods are calculated by the generalized method using the calculated mass flow rate. Specifically, the inlet Mach number is obtained from the inlet pressure and temperature as well as the mass flow rate. Then the generalized steady flow equation (21) is solved to obtain the Mach number at every flow cell. Next, the pressure and temperature at every cell inside the flow path are calculated from equations (22) and (23). This way, if the mass flow rate calculated is correct, the Mach number, pressure and temperature should also be correct for steady flows. Note that, unlike the generalized method, no iteration is needed since the mass flow rate is calculated separately before the generalized steady equation is solved.

RESULTS

Most of the results shown in this paper are from test problems where the inlet stagnation pressure and temperature as well as the outlet pressure are know. The area of the pipe as well as the magnitudes of friction, heat transfer, and mass addition are also specified. The Mach number, pressure and temperature inside the pipe are calculated using various methods discussed above. The gas in all test problems is assumed to be perfect gas with a specific heat ratio of 1.4 and gas constant of 287 m^2/s^2-K.

Steady Flow with Area Change

The following adiabatic frictionless steady flow problem with no mass addition is considered in this section. Air at stagnation pressure of 0.1215 MPa and temperature of 368.34 K enters a nozzle having a cross-section area of

$$A = \frac{C_3}{C_0 x + C_2} \tag{31}$$

The axial distance of the nozzle is from x=0 to x=20 m. The constants C_3=1 and C_2=100. Two cases are studied: (1) C_0 =1 and outlet pressure of 84.63 kPa for the converging nozzle and (2) C_0=-1 and outlet pressure of 132.41 kPa for the diverging nozzle.

The Mach number and pressure distribution inside the converging nozzle predicted by isentropic, ORING2, Lapple and generalized methods are compared with the exact solution in Figure 6 and Figure 7, respectively. Note that a discharge coefficient of unity is applied for the isentropic method. It is evident that the predict Mach number and pressure from isentropic method, ORING2, and generalized methods agree very well with the exact solution. For the Lapple method, the predicted Mach number is slightly smaller whereas the pressure is slightly larger than the exact solution because of the lower predicted mass flow rate as suggested in Figure 3.

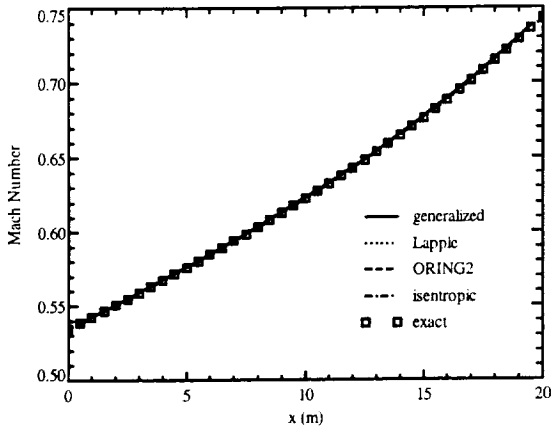

Figure 6: Comparison of Mach number predicted from different methods with the exact solution.

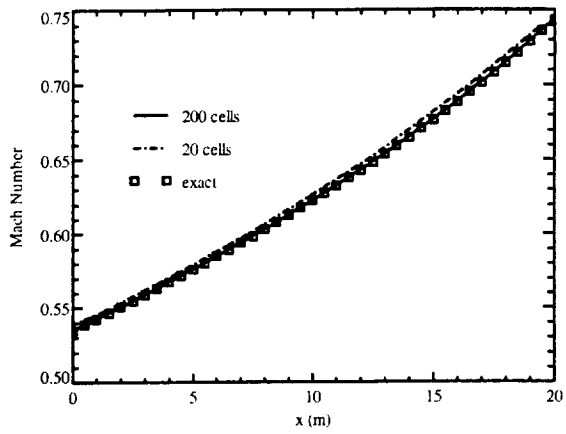

Figure 8: Comparison of Mach number predicted from SHARP with different number of cells and the exact solution.

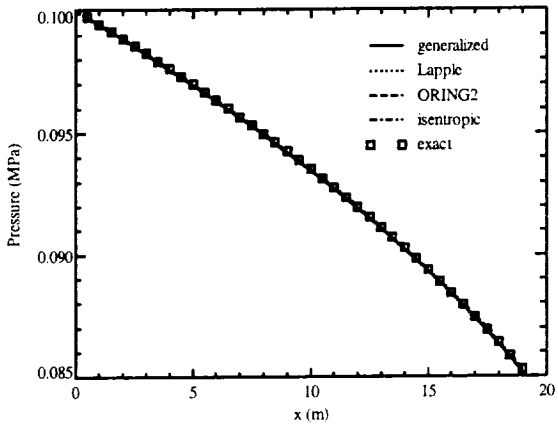

Figure 7: Comparison of pressure predicted from different methods with the exact solution.

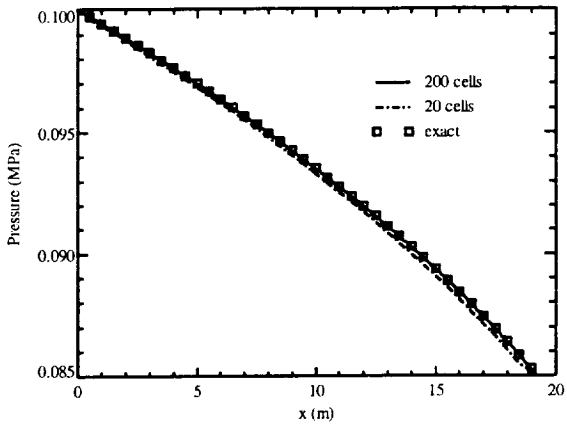

Figure 9: Comparison of pressure predicted from SHARP with different number of cells and the exact solution.

Figure 8 and Figure 9 show the Mach number and pressure distribution for the converging nozzle predicted by the SHARP method, respectively, together with the exact solution. The predicted Mach number and pressure using 200 flow cells agree very well with the exact solution whereas the predictions with 20 cells are not as good.

The Mach number and pressure distribution for the diverging nozzle predicted by isentropic, ORING2, Lapple and generalized methods are compared with the exact solution in Figure 10 and Figure 11, respectively. The predicted Mach number and pressure by these methods agree very well with the exact solution. Similar to the converging nozzle, the predicted Mach number from the Lapple method is smaller whereas the pressure is larger than the exact solution because of the lower mass flow rate as suggested in Figure 3. However, the discrepancy between the Lapple prediction and exact solution is much larger for the diverging nozzle than the converging nozzle because the pressure ratio p_b/p_0 is

much closer to unity.

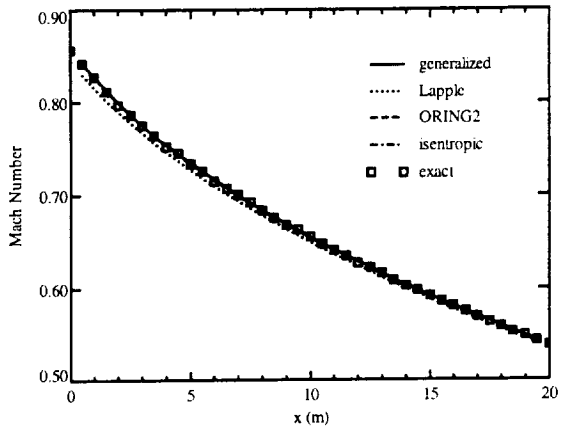

Figure 10: Comparison of Mach number predicted from different methods with the exact solution for the diverging nozzle.

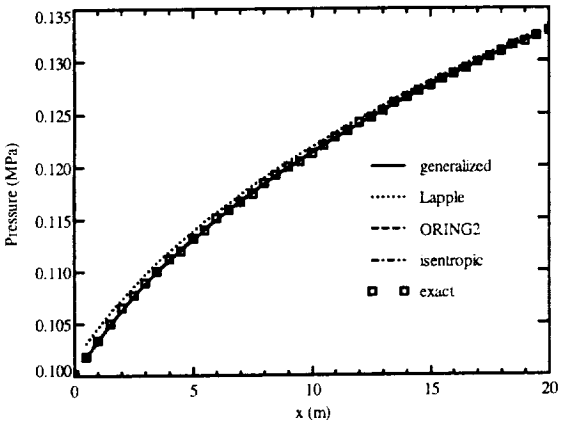

Figure 11: Comparison of pressure predicted from different methods with the exact solution for the diverging nozzle.

Figure 12 and Figure 13 show the Mach number and pressure distribution for the diverging nozzle predicted by the SHARP method, respectively. Similar to the diverging nozzle, the predicted Mach number and pressure using 200 flow cells agree very well with the exact solution whereas the predictions with 20 cells are not as good. That is, more flow cells are usually required to obtain accurate results using SHARP than other methods.

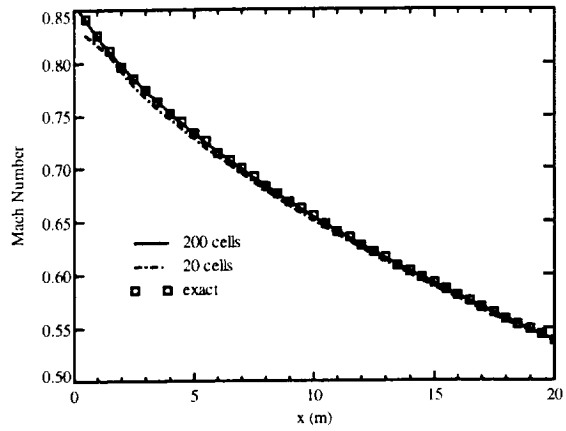

Figure 12: Comparison of Mach number predicted from SHARP with different number of cells and the exact solution for the diverging nozzle.

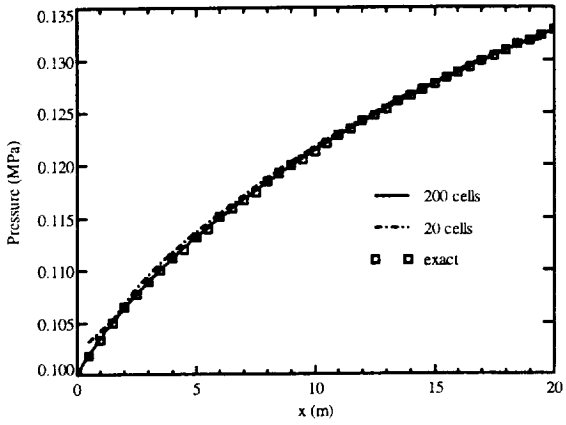

Figure 13: Comparison of pressure predicted from SHARP with different number of cells and the exact solution for the diverging nozzle.

Steady Flow with Friction

The following adiabatic steady flow problem with no area change and no mass addition is considered in this section. Air enters a pipe at a stagnation pressure of 0.1007 MPa and temperature of 300.6 K. This pipe has a diameter of 0.1 m, length of 274.385 m, and friction factor of 0.024. The pressure at the pipe exit is 19.54 kPa.

The Mach number and pressure distribution predicted by SHARP, ORING2, Lapple and generalized methods are compared with the exact solution in Figure 14 and Figure 15, respectively. It is evident that the predict

Mach number and pressure from SHARP and generalized methods agree very well with the exact solution. However, the Lapple method overpredicts the Mach number and underpredicts the pressure whereas the ORING2 method underpredicts the Mach number and overpredicts the pressure. This is consistent with the fact that Lapple method predicts a higher mass flow rate than the ORING2 method as discussed in Figure 4 and Figure 5.

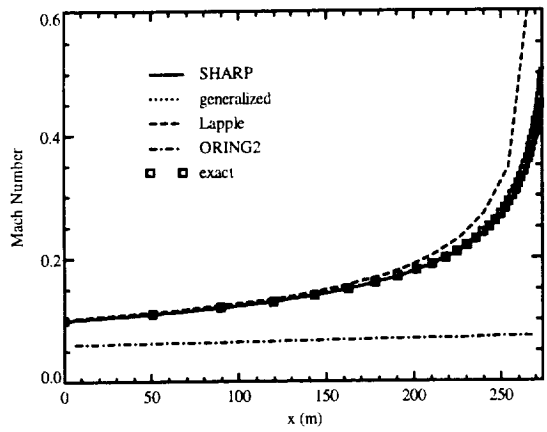

Figure 14: Comparison of Mach number predicted from different methods with the exact solution.

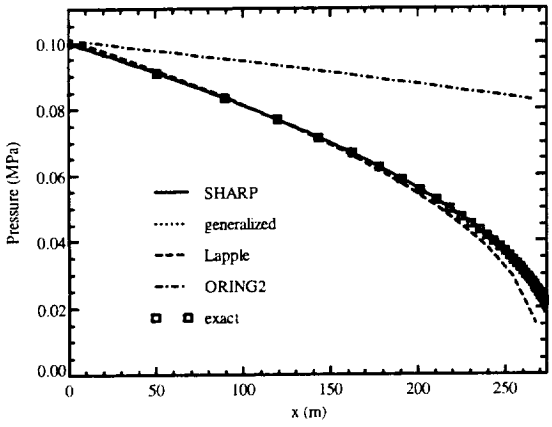

Figure 15: Comparison of pressure predicted from different methods with the exact solution.

Figure 16 and Figure 17 show the Mach number and pressure distribution predicted by the isentropic method, respectively. Since this method does not take into account the effect of friction when the mass flow rate is calculated, a discharge coefficient smaller than unity should be applied to obtain the correct mass flow rate. For this case, the optimal discharge coefficient is 0.172. A discharge coefficient smaller than this value predicts smaller Mach number and larger pressure whereas a discharge coefficient larger than this value predicts larger Mach number and smaller pressure.

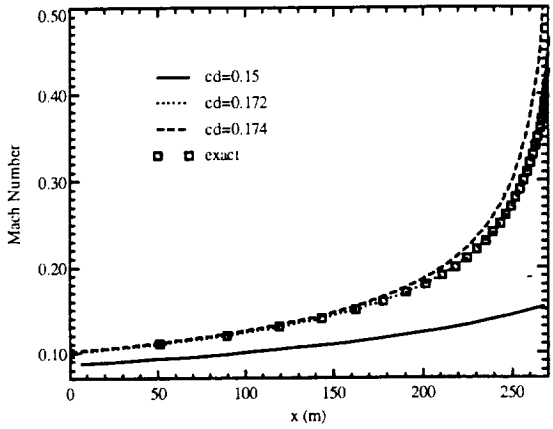

Figure 16: Comparison of Mach number predicted from the isentropic method with different discharge coefficients and the exact solution.

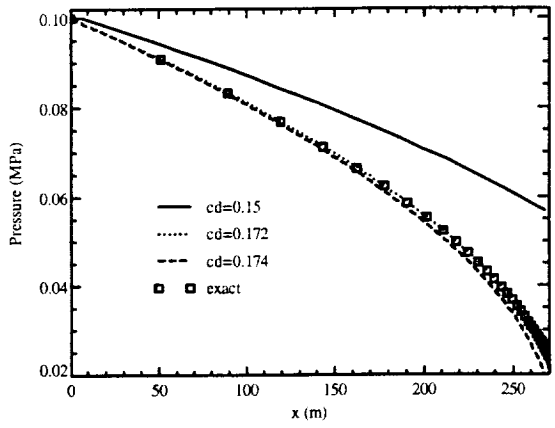

Figure 17: Comparison of pressure predicted from the isentropic method with different discharge coefficients and the exact solution.

Steady Flow with Heat Transfer

The following frictionless steady flow problem with no area change and no mass addition is considered in this section. Heat is added to a pipe with a diameter of 0.01 m and length of 20 m at a rate of 200 J/m. Air enters this pipe at a stagnation pressure of 0.1007 MPa and temperature of 300.6 K. The pressure at the pipe exit is

93.73 kPa. This problem is solved using all the five methods and the pressure and Mach number inside the pipe are compared with the exact solutions.

The Mach number and pressure distribution predicted by SHARP, ORING2, Lapple and generalized methods are compared with the exact solution in Figure 18 and Figure 19, respectively. The predict Mach number and pressure from SHARP and generalized methods agree very well with the exact solution. Both Lapple and ORING2 methods overpredict the Mach number and underpredict the pressure because the effects of heat addition is not considered and the predicted mass flow rate from these two methods is much larger.

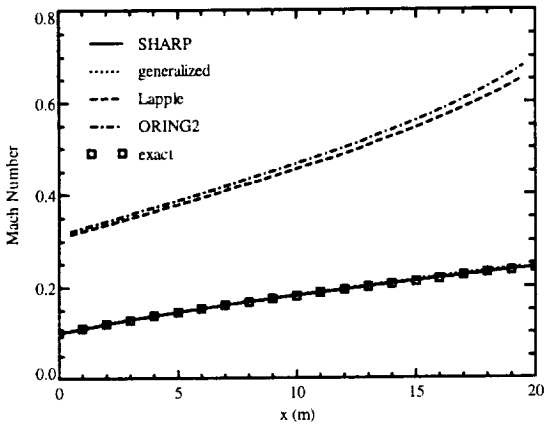

Figure 18: Comparison of Mach number predicted from different methods with the exact solution.

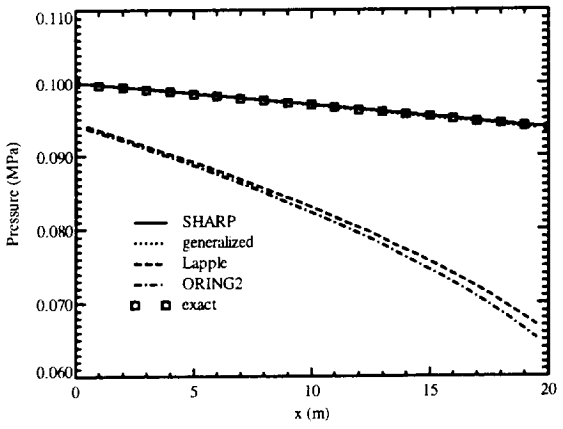

Figure 19: Comparison of pressure predicted from different methods with the exact solution.

Figure 20 and Figure 21 show the Mach number and pressure distribution predicted by the isentropic method, respectively, together with the exact solution. Since this method does not take into account the effect of heat addition when calculating mass flow rate, a discharge coefficient smaller than unity should be applied to obtain the correct mass flow rate. For this case, the optimal discharge coefficient is 0.034. A discharge coefficient smaller than this value predicts smaller Mach number and larger pressure whereas a discharge coefficient larger than this value predicts larger Mach number and smaller pressure.

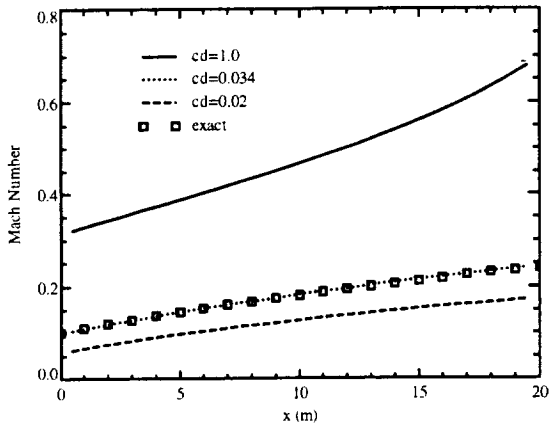

Figure 20: Comparison of Mach number predicted from the isentropic method with different discharge coefficients and the exact solution.

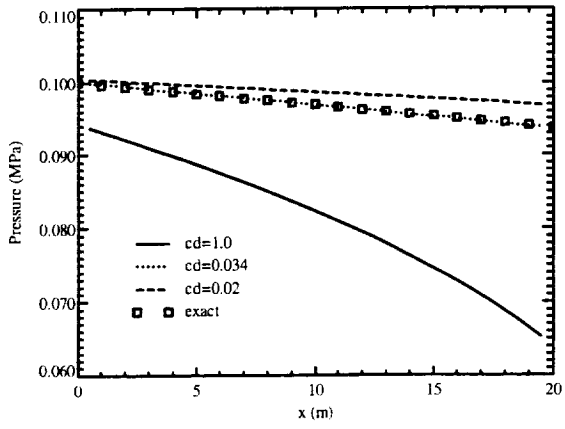

Figure 21: Comparison of pressure predicted from the isentropic method with different discharge coefficients and the exact solution.

Steady Flow with Mass Addition

The following adiabatic frictionless steady flow problem with no area change is considered in this section. Air at the same temperature as the air inside is added to a pipe with a diameter of 0.1 m and length of 20 m at a rate of 0.5 kg/s-m. Air enters this pipe at a stagnation pressure of 0.1007 MPa and temperature of 300.6 K. The pressure at the pipe exit is 91.34 kPa.

The Mach number and pressure distribution predicted by SHARP, ORING2, Lapple and generalized methods are compared with the exact solution in Figure 22 and Figure 23, respectively. The predict Mach number and pressure from SHARP and generalized methods agree very well with the exact solution. Both Lapple and ORING2 methods overpredict the Mach number and underpredict the pressure because the effects of mass addition is not taken into account and the predicted mass flow rate from these two methods is much larger.

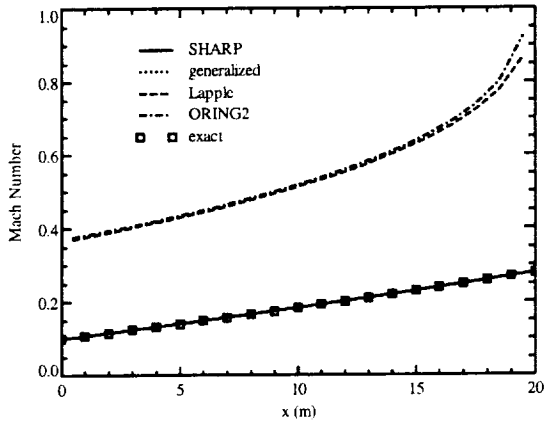

Figure 22: Comparison of Mach number predicted from different methods with the exact solution.

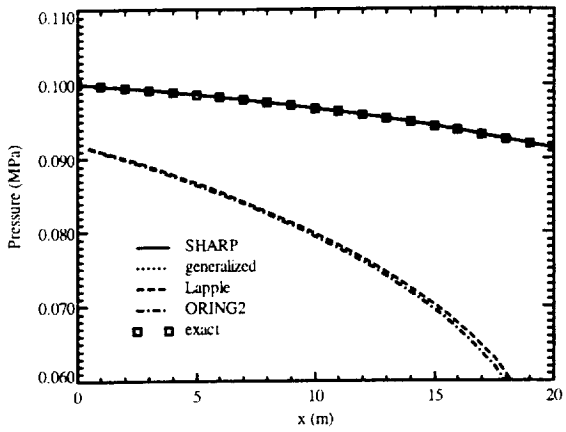

Figure 23: Comparison of pressure predicted from different methods with the exact solution.

Figure 24 and Figure 25 show the Mach number and pressure distribution predicted by the isentropic method, respectively, together with the exact solution. Since this method does not take into account the effect of mass addition when calculating mass flow rate, a discharge coefficient smaller than unity should be applied to obtain the correct mass flow rate. For this case, the optimal discharge coefficient is 0.03. A discharge coefficient smaller than this value predicts smaller Mach number and larger pressure whereas a discharge coefficient larger than this value predicts larger Mach number and smaller pressure.

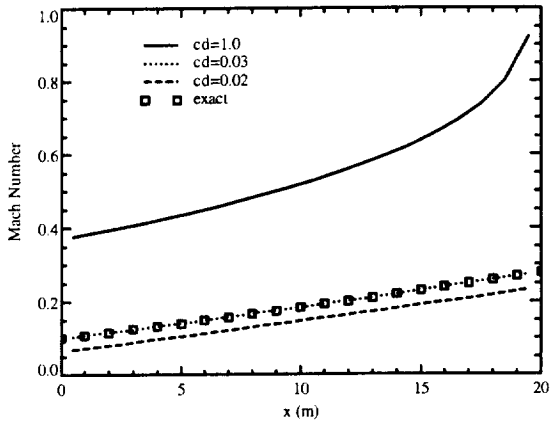

Figure 24: Comparison of Mach number predicted from the isentropic method with different discharge coefficients and the exact solution.

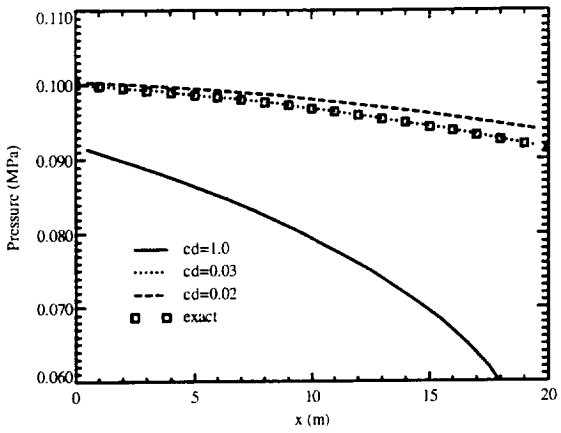

Figure 25: Comparison of pressure predicted from the isentropic method with different discharge coefficients and the exact solution.

Transient Flow with Area Change

All the test cases shown above are steady flow problems and only the SFLOW predictions at long times were compared with the exact steady-state solution. In this and the following two sections, the various flow solvers are assessed using one-dimensional unsteady flow problems with analytical solutions derived by Cai[14].

It can be shown that for one-dimensional adiabatic frictionless compressible flow in a nozzle with a cross-section area shown in equation (31), one exact solution of the governing equation is

$$\begin{aligned} p &= const \\ \rho &= const \\ u &= \frac{2C_0(C_0 x + C_2)}{2C_0^2 t + C_1} \end{aligned} \tag{32}$$

if there is no mass addition. Similar to the steady flow with area change problems discussed above, two cases are studied: (1) a converging nozzle with C_0 =1 and (2) a diverging nozzle with C_0=-1. For both cases, the gas is air with a static pressure of 0.1 MPa and temperature of 300 K. The stagnation pressure and temperature as well as the static pressure at the nozzle outlet are specified whereas the velocity and pressure inside the nozzle are calculated.

The governing equation for this transient flow problem with area change only is

$$\frac{\partial u}{\partial t} + u\frac{\partial u}{\partial x} + \frac{1}{\rho}\frac{\partial p}{\partial x} = 0 \tag{33}$$

In this problem, the pressure is constant and the term $u\partial u/\partial x$ is balanced by $\partial u/\partial t$. For isentropic, ORING2, Lapple and generalized methods, however, steady state (i.e., $\partial u/\partial t$=0) is assumed and the pressure term has to be nozero to balance $u\partial u/\partial x$. For the converging nozzle, $u\partial u/\partial x$ >0 and the outlet pressure predicted from these methods will be smaller than the predicted inlet pressure whereas the predicted outlet pressure for the diverging nozzle will be larger than the predicted inlet pressure since $u\partial u/\partial x$ <0.

The velocity at the inlet and outlet from ORING2, Lapple, SHARP, and generalized methods are compared with the exact solution in Figure 26 and Figure 27, respectively, for the converging nozzle problem. The velocity predicted by SHARP method agrees very well with the exact solution whereas ORING2 and generalized methods predict a much smaller velocity. Note that the generalized method and the ORING2 method predict the same velocity since there are no friction, heat transfer and mass addition in this problem. The Lapple method predicts even smaller velocity than ORING2 and generalized methods at later times when the pressure ratio is closer to unity, consistent with the smaller predicted mass flow rate by the Lapple method shown in Figure 3.

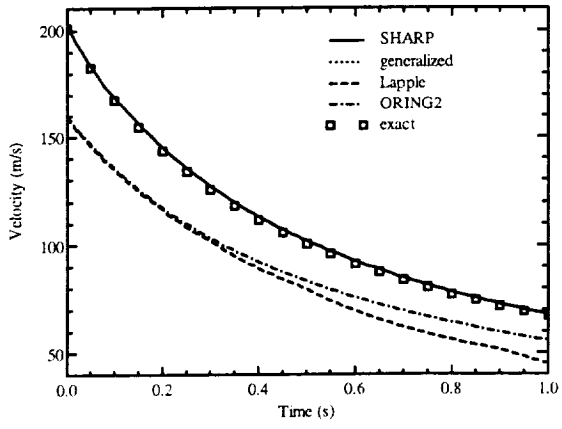

Figure 26: Comparison of inlet velocity predicted by various flow solvers with the exact solution.

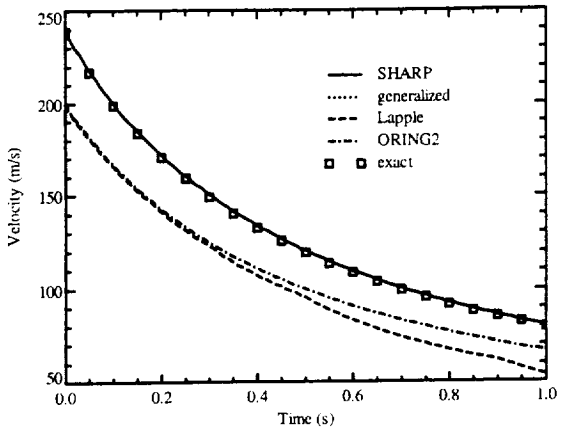

Figure 27: Comparison of outlet velocity predicted by various flow solvers with the exact solution.

Figure 28 shows the comparison of inlet and outlet pressure predicted by SHARP and generalized methods with the exact solution. The pressure predicted by SHARP method agrees very well with the exact solution. For the generalized method, the outlet pressure agrees well with the exact solution but the inlet pressure is much larger, consistent with the above analysis using equation (33). Although not shown here, the isentropic, ORING2, and Lapple methods predict qualitatively similar pressure with the generalized method.

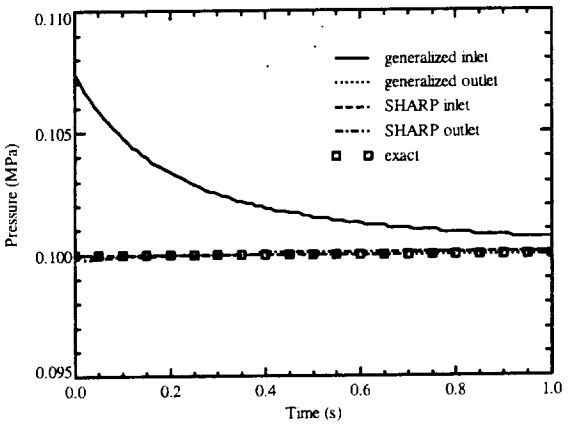

Figure 28: Comparison of inlet and outlet pressure predicted by SHARP and generalized methods with the exact solution.

Figure 29 and Figure 30 show the velocity at the inlet and outlet from the isentropic method compared with the exact solution. As expected, the predicted velocity is larger for larger discharge coefficient. Unlike the steady-state problems, however, there is no single value of discharge coefficient which matches the exact velocity. A time dependent discharge coefficient near 1.15 could be used to match the outlet velocity at different times, but the predicted inlet velocity using this discharge coefficient is much smaller than the exact solution.

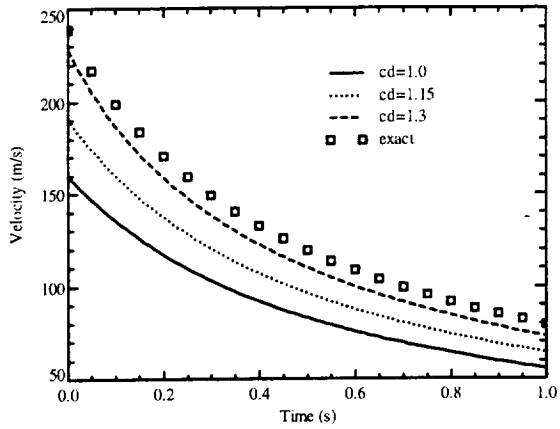

Figure 29: Comparison of inlet velocity predicted from the isentropic method with different discharge coefficients and the exact solution.

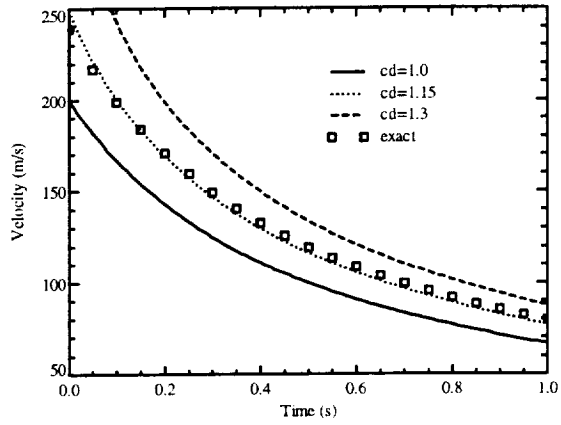

Figure 30: *Comparison of outlet velocity predicted from the isentropic method with different discharge coefficients and the exact solution.*

The velocity at the inlet and outlet from ORING2, Lapple, SHARP, and generalized methods are compared with the exact solution in Figure 31 and Figure 32, respectively, for the diverging nozzle problem. Similar to the converging nozzle problem, the velocity predicted by SHARP method agrees very well with the exact

solution. ORING2, Lapple, and generalized methods, however, predict a much larger velocity in contrast to the smaller velocity predicted for the converging nozzle.

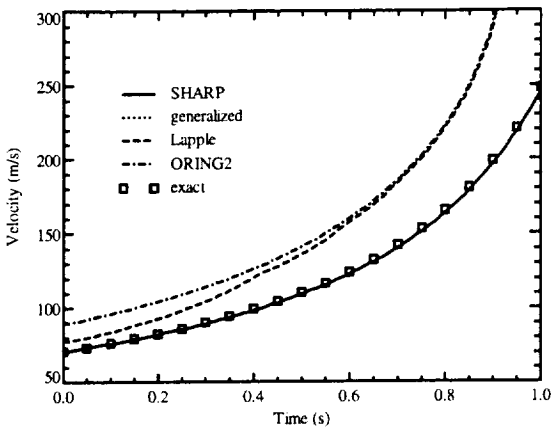

Figure 31: Comparison of inlet velocity predicted by various flow solvers with the exact solution for the diverging nozzle.

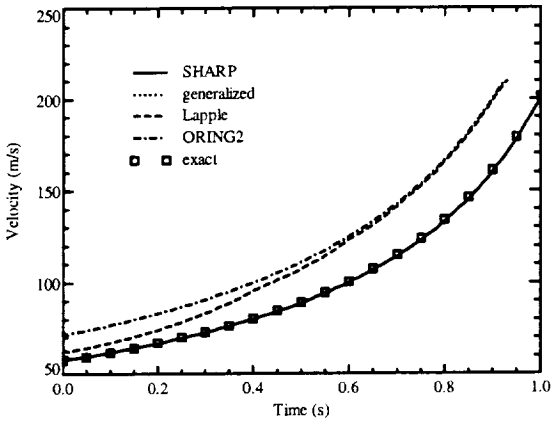

Figure 32: Comparison of outlet velocity predicted by various flow solvers with the exact solution for the diverging nozzle.

Figure 33 shows the comparison of inlet and outlet pressure predicted by SHARP and generalized methods with the exact solution. The pressure predicted by SHARP method agrees very well with the exact solution. For the generalized method, the outlet pressure agrees well with the exact solution but the inlet pressure is much smaller, consistent with the above analysis using equation (33). Although not shown here, the isentropic, ORING2, and Lapple methods predict similar pressure as the generalized method.

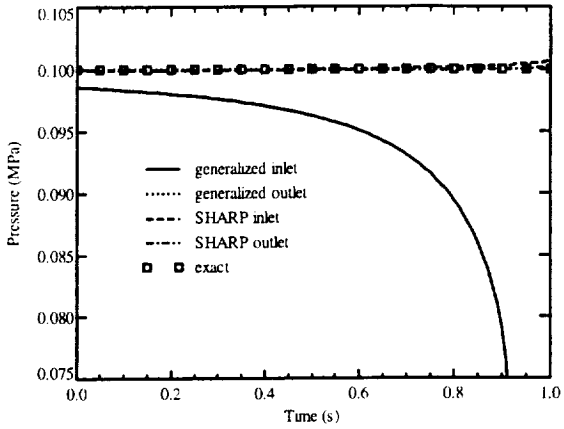

Figure 33: Comparison of inlet and outlet pressure predicted by SHARP and generalized methods with the exact solution for the diverging nozzle.

Figure 34 and Figure 35 show the velocity at the inlet and outlet from the isentropic method compared with the exact solution. As expected, the predicted velocity is larger for larger discharge coefficient. Unlike the steady-state problems, however, there is no single value of discharge coefficient which matches the exact velocity. A time dependent discharge coefficient near 0.8 could be used to match the outlet velocity at different times, but the predicted inlet velocity using this discharge coefficient will not match the exact solution.

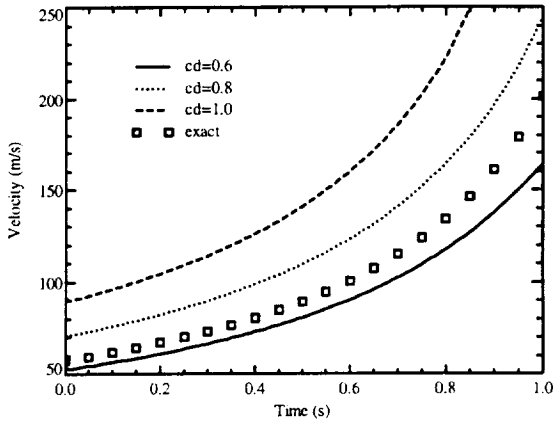

Figure 34: Comparison of inlet velocity predicted from the isentropic method with different discharge coefficients and the exact solution for the diverging nozzle.

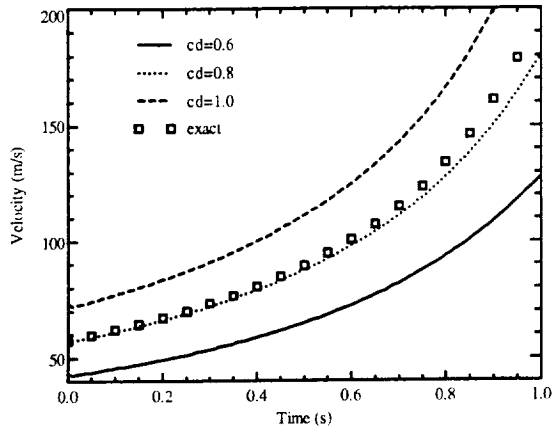

Figure 35: Comparison of outlet velocity predicted from the isentropic method with different discharge coefficients and the exact solution for the diverging nozzle.

Transient Flow with Heat Transfer

It can be shown that for one-dimensional frictionless compressible flow in a circular pipe with a heat transfer rate per unit mass of

$$q = \frac{\gamma}{\gamma - 1}\frac{C_1 p}{C_5}\left(\frac{C_1 x + C_3}{C_1 t + C_2}\right)^{1+C_4/C_1} \tag{34}$$

the exact solution of the governing equation is

$$\begin{aligned} p &= const \\ \rho &= \frac{C_5 (C_1 t + C_2)^{C_4/C_1}}{(C_1 x + C_3)^{1+C_4/C_1}} \\ u &= \frac{C_1 x + C_3}{C_1 t + C_2} \end{aligned} \tag{35}$$

if the cross-section area is constant and there is no mass addition. This transient flow with heat transfer case was simulated using various flow solvers by assuming C_1= C_4=1, C_3= C_5=5000 and C_2=15. The flow path is from x=0 to x=20 m. The gas is air with a static pressure of 0.1 MPa. The stagnation pressure and temperature as well as the static pressure at the nozzle outlet are specified as input whereas the velocity and pressure inside the pipe are calculated.

Figure 36 to Figure 40 show the comparison of inlet and outlet Mach number predicted by the five flow solvers with the exact solution. The predicted Mach number from SHARP agrees very well with the exact solution whereas those from Lapple and generalized methods do not agree well. For ORING2 and isentropic methods with a discharge coefficient of 1.0, the predicted inlet Mach number agree well with the exact solution but the predicted outlet Mach number is larger. No optimal discharge coefficient exists for the isentropic method which predicts Mach number in good agreement with the exact solution at all locations and times.

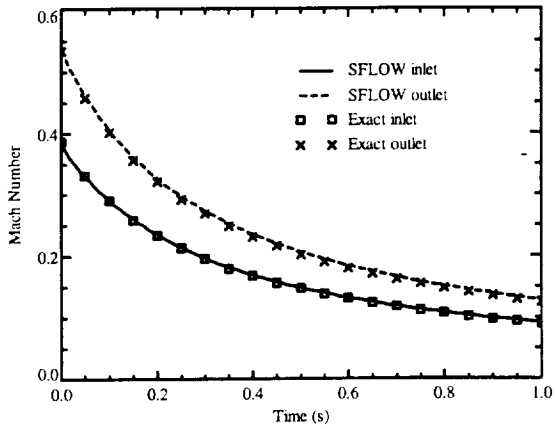

Figure 36: Comparison of inlet and outlet Mach number predicted from the SHARP method with the exact solution.

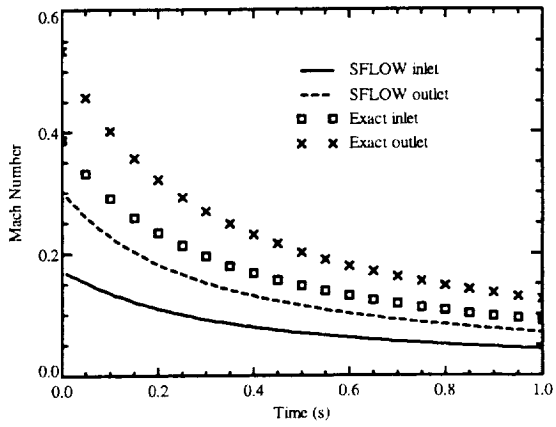

Figure 37: Comparison of inlet and outlet Mach number predicted from the generalized method with the exact solution.

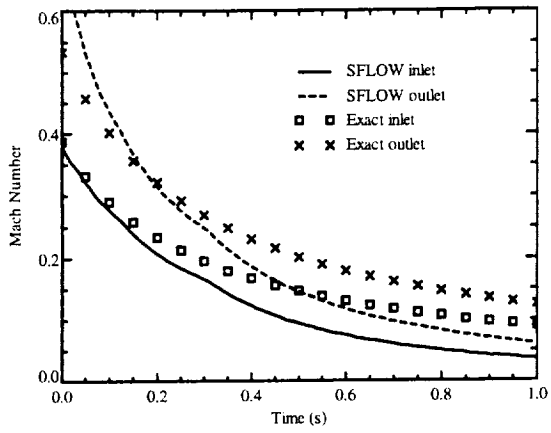

Figure 38: Comparison of inlet and outlet Mach number predicted from the Lapple method with the exact solution.

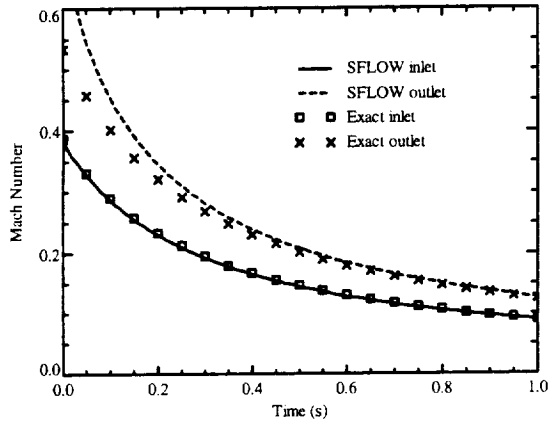

Figure 39: Comparison of inlet and outlet Mach number predicted from the ORING2 method with the exact solution.

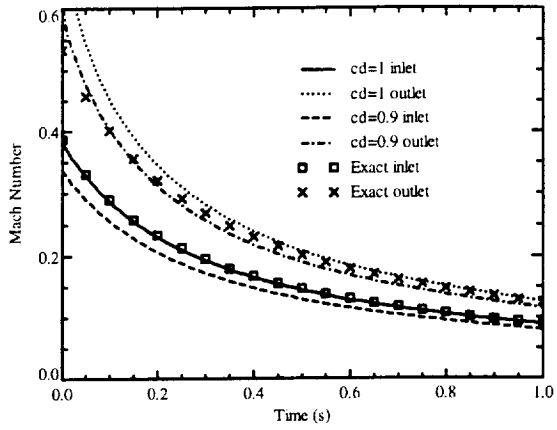

Figure 40: Comparison of inlet and outlet Mach number predicted from isentropic method with different discharge coefficients and the exact solution.

Transient Flow with Area change, Friction, and Heat Transfer

For one-dimensional compressible flow in a circular pipe with area A, friction factor f, and heat transfer rate q given by

$$A = \frac{1}{C_4 \exp\left(-\sqrt{\pi / C_1}\, x\right) + \sqrt{C_x / \pi}} \tag{36}$$

$$f = \frac{4}{\sqrt{C_1\left(C_4 \exp\left(-\sqrt{\pi / C_1}\, x\right) + \sqrt{C_x / \pi}\right)}} \tag{37}$$

$$q = -\sqrt{\frac{\pi}{C_1}}\left(\frac{C_2\left(C_4 \exp\left(-\sqrt{\pi / C_1}\, x\right) + \sqrt{C_x / \pi}\right)}{C_2 t + C_3}\right)^3 \tag{38}$$

the exact solution is

$$p = const$$
$$\rho = const$$
$$u = \frac{C_2\left(C_4 \exp\left(-\sqrt{\pi / C_1}\, x\right) + \sqrt{C_x / \pi}\right)}{C_2 t + C_3} \tag{39}$$

if there is no mass addition. This transient flow with area change, friction, and heat transfer case is simulated using SFLOW by assuming $C_0 = C_3 = C_4 = 1$, $C_1 = 1000$, and $C_2 = 15$. The flow path is from $x=0$ to $x=20$ m. The gas is air with a static pressure of 0.1 MPa and temperature of 300 K. The stagnation pressure and

temperature as well as the static pressure at the nozzle outlet are specified as input whereas the velocity and pressure inside the pipe are calculated.

The predicted velocity at the inlet is compared with the exact solution in Figure 41. A very good agreement is obtained for the SHARP method whereas the predicted velocities from ORING2, Lapple and generalized methods are much smaller.

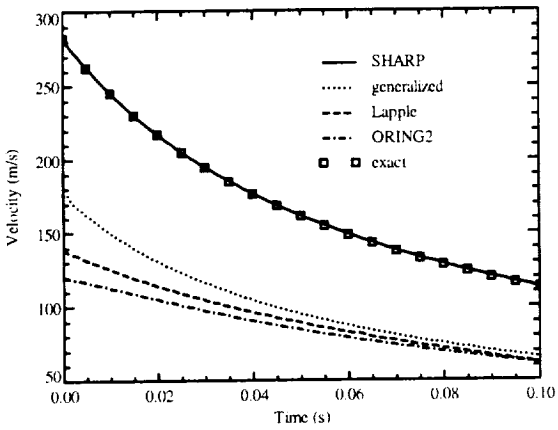

Figure 41: Comparison of predicted inlet velocity with the exact solution.

Volume Filling

All the test problems discussed above focus on calculating flow properties inside a flow path with specified inlet stagnation pressure and temperature, as well as static pressure at the path exit. A volume filling problem is studied in this section where the mass flow rate is calculated similar to the problems discussed above and the pressure and temperature in the tank are calculated by mass and energy conservation laws using the mass flow rate at the pipe inlet and outlet[3]. Specifically, air at a pressure of 1,000 psia and temperature of 5,400 R fills a tank with a volume of 100 in^3. The tank initial pressure and temperature is 14.7 psia and 540 R. The area of the flow path is 0.0235 in^2.

Figure 42 shows the predicted volume pressure in comparison with the exact solution. A discharge coefficient of 1.0 is used for the isentropic method. The volume pressure predicted by isentropic, ORING2, Lapple and generalized methods agree very well with the exact solution whereas that from SHARP is smaller. This is because the exact solution is derived by assuming the flow is quasi-steady (i.e., steady state is assumed when the mass flow rate is calculate at every time step) but SHARP treats the flow as transient.

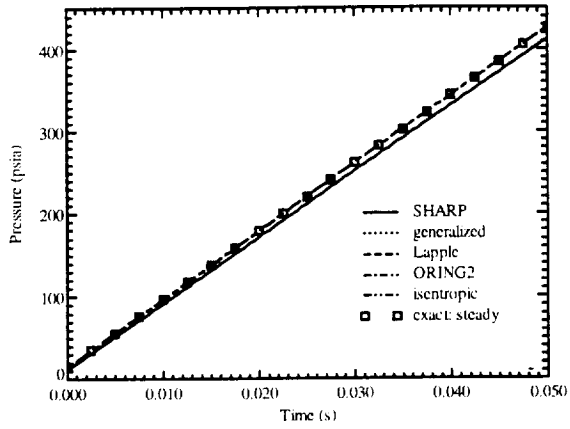

Figure 42: Comparison of predicted tank pressure with the exact solution derived by assuming the flow is quasi-steady.

CONCLUSIONS

The capability of various flow solvers in predicting transient compressible flow phenomena with area change, friction, heat transfer, and mass addition has been assessed. Specifically, the following flow solvers have been studies in detail: isentropic method, ORING2 method, Lapple method, generalized method, and SHARP method. Of the five solvers, only SHARP is designed for transient flow problems whereas all other solvers assume the flow is quasi-steady. The isentropic method only considers the effect of area change and applies a discharge coefficient to take into account the effects of friction, heat transfer, and mass addition. Both ORING2 and Lapple methods try to take into account the effects of friction, but heat transfer and mass addition are neglected when the mass flow rate is calculated. The generalized method considers area change, friction, heat transfer as well as mass addition.

SHARP method is the most accurate among the five flow solvers studied in this paper. The results from SHARP agree very well with the exact solution for all test problems shown in this paper except the volume filling problem where the exact solution is derived by assuming the flow is quasi-steady.

The generalized method is capable of accurately solving all steady flow problems with area change, friction, heat transfer and mass addition. However, the results from

this method are not accurate for transient flow problems because steady state is assumed when the pressure, temperature and Mach number inside the flow path are calculated.

Both ORING2 and Lapple methods predict accurate results for steady flows with area change only. For transient flows or flows with heat transfer or mass addition, however, these two methods are not accurate. Although these methods try to take into account the effects of friction, it is accurate only when the friction is small enough.

For steady flows with area change only, the isentropic method predicts accurate results using a constant discharge coefficient of 1.0. For steady flows with friction, heat transfer, or mass addition, a unique discharge coefficient can be found such that the prediction agrees well with the exact solution. However, this optimal discharge coefficient is not known before the calculation. Note that, while friction makes the optimal discharge coefficient smaller, heat transfer and mass addition could increase or decrease the optimal discharge coefficient depending on whether the heat transfer is from the gas or to the gas and whether it is mass addition or removal. For transient flow problems, there is no optimal discharge coefficient which makes the prediction by the isentropic method agree well with the exact solution at all locations and times.

REFERENCE

1. Laubacher, B.A., Eaton, A.M., Pate, R.A., Wang, Q., Mathias, E.C. and Shipley, J.L. 1999 "Cold-flow simulation and CFD modeling of the space shuttle solid rocket motor nozzle joints," AIAA Paper 99-2793.

2. Eaton A.M. and Mathias, E. 2000 "Simulating heat transfer to a solid rocket motor nozzle-case-joint thermal barrier," AIAA Paper 2000-3807.

3. Wang, Q., Mathias, E.C., Heman, J.R. and Smith, C.W. 2000 "A thermal-flow code for modeling gas dynamics and heat transfer in space shuttle solid rocket motor joints," AIAA Paper 2000-3189.

4. Wang, Q., Ewing, M.E., Mathias, E.C., Smith, C. and Heman, J. 2001 "Development of flow and heat transfer models for the carbon fiber rope in nozzle joints of the space shuttle reusable solid rocket motor," AIAA Paper 2001-3441.

5. Clayton, J.L. 1989 "Modeling of the space shuttle solid rocket motor nozzle boot cavity pressurization process," J. Spacecraft, Vol. 26, pp. 385-390.

6. Clayton, J.L. 1999 "Reusable solid rocket motor nozzle joint-4 test correlated gas dynamics-thermal analysis," AIAA Paper 99-2791.

7. Network Analysis Inc. 1996 SINDA/G User's Guide, Tempe, AZ.

8. O'Malley, M.J. 1988 "A model for predicting RSRM joint volume pressurization, temperature transients, and ablation," AIAA Paper 88-3332.

9. Zucrow, M.J. and Hoffman, J.D. 1976 Gas Dynamics, John Wiley & Sons, Inc., New York.

10. Lapple, C.E. 1943 "Isothermal and adiabatic flow of compressible fluids," Transcripts from American Institute of Chemical Engineers, Vol. 39, pp. 385-432.

11. Golafshani, M. and Loh, H.T. 1989 "Computation of two-phase viscous flow in solid rocket motors using a flux-split Eulerian-Lagrangian technique," AIAA Paper 89-2785.

12. Loh, H.T. and Golafshani, M. 1990 "Computation of viscous chemically reacting flows in hybrid rocket motors using an upwind LU-SSOR scheme," AIAA Paper 90-1570.

13. Loh, H.T., Smith-Kent, R., Perkins, F and Chwalowski, P. 1996 "Evaluation of aft skirt length effects on rocket motor base heat using computational fluid dynamics," AIAA Paper 96-2645.

14. Cai, R. 1998 "Some explicit analytical solutions of unsteady compressible flow," Journal of Fluid Eng., Vol. 120, pp. 760-764.